Crystallization Behavior of Carbon Nanotubes-Filled Polyamide 1010

Biao Wang,[1] Guangping Sun,[1] Jingjiang Liu,[2] Xiaofeng He,[1] Jing Li[2]

[1]*The Key Laboratory of Automobile Material of Ministry of Education and Department of Materials Science and Engineering, Jilin University, Changchun 130025, People's Republic of China*
[2]*State Key Laboratory of Polymer Physics and Chemistry, Changchun Institute of Applied Chemistry, Chinese Academy of Sciences, Changchun 130022, People's Republic of China*

Received 23 May 2005; accepted 27 October 2005
DOI 10.1002/app.23805
Published online in Wiley InterScience (www.interscience.wiley.com).

ABSTRACT: The nanocomposites of polyamide1010 (PA1010) filled with carbon nanotubes (CNTs) were prepared by melt mixing techniques. The isothermal melt-crystallization kinetics and nonisothermal crystallization behavior of CNTs/PA1010 nanocomposites were investigated by differential scanning calorimetry. The peak temperature, melting point, half-time of crystallization, enthalpy of crystallization, etc. were measured. Two stages of crystallization are observed, including primary crystallization and secondary crystallization. The isothermal crystallization was also described according to Avrami's approach. It has been shown that the addition of CNTs causes a remarkable increase in the overall crystallization rate of PA1010 and affects the mechanism of nucleation and growth of PA1010 crystals. The analysis of kinetic data according to nucleation theories shows that the increment in crystallization rate of CNTs/PA1010 composites results from the decrease in lateral surface free energy. © 2006 Wiley Periodicals, Inc. J Appl Polym Sci 100: 3794–3800, 2006

Key words: polyamide1010; carbon nanotube; DSC; crystallization

INTRODUCTION

The discovery of carbon nanotube (CNT) has inspired scientists to do extensive studies.[1–3] A CNT has a unique atomic structure, which is a single sheet of graphite rolled into a cylinder several micrometers in length and a few nanometers in diameter. Nanotubes can take two forms, i.e., single-walled and multi-walled. Single-walled nanotubes consist of one layer of carbon atoms through the thickness of cylinder wall. Multi-walled CNTs, which were the first to be discovered, consist of concentric cylinders around a common central hollow. Both forms of CNTs show remarkable mechanical and physical properties, such as high stiffness, strength, and conductivity, because of their particular topological structure, high aspect ratio, and large surface area. These preponderant performances of CNTs have attracted wide and considerable attention in application in polymer/CNTs nanocomposites.[4–6]

Among the most versatile polymer matrices, polyamide is one class of important engineering thermoplastics, which is the most widely used because of its high strength, elasticity, toughness, and abrasion resistance. Poly(iminosebacoyl iminodecamethylene), (PA1010), which is an extraordinary semicrystalline polyamide, is especially manufactured commercially in China. Except for the common features, it has a notable resistance to moisture when compared with polyamide 6,6. Mo and coworkers report the crystalline structure and thermodynamic parameters of PA1010, PA1010 crystallization in the triclinic system, with the following lattice dimensions: $a = 0.49$ nm, $b = 0.54$ nm, $c = 2.78$ nm, $\alpha = 49°$, $\beta = 77°$, and $\gamma = 63.5°$.[7]

The microstructure of polymer composites depends on applied fillers. For example, poly(vinylidene-fluoride) has a strong α-nucleating effect on iPP,[8] and an amorphous immiscible polymer ethylene-propylene-dieneterpolymer affects the crystalline behavior and structure of PP.[9] Some inorganic fillers (glass fibers, clay, calcium carbonate, carbon black, etc.), as reinforcing agents in polymer composites, can usually induce nucleation for crystallization of matrix.[10–13] However, at present, CNTs-induced polymer crystallization has rarely been investigated, in addition to mainly CNTs-filled polypropylene.[14–17] In this work, the influence of CNTs on the crystallization of PA1010 was studied by means of differential scanning calorimetry.

EXPERIMENTAL

Polyamide 1010 was commercially supplied by Shijinggou Union Chemical Co., Jilin, China. Its melting

Correspondence to: J.J. Liu. (jjliu@ciac.jl.cn).
Contract grant sponsor: Chinese Nation Science Foundation; contract grant number: 50403006.

TABLE I
The Characteristics of the Carbon Nanotubes

Carbon nanotube	Diameter (nm)	Length (μm)	Purity (%)	Ash mass fraction (%)	Special-surface area (m^2/g)	Amorphous-carbon (%)
MWNTs	10–30	0.5–40	≥95	≤0.2	40–300	<3
SWNTs	<2	0.5–50	≥45	≤2	>600	<5
MWNTs-carboxylic	10–30	0.5–40	≥95	≤0.2	40–300	<3

flow rate is 10 g/10 min, and its chemical structure is shown as follows:

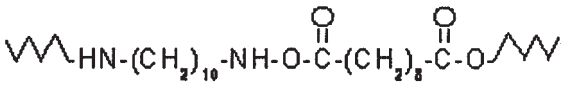

The CNT used was multi-walled carbon nanotube (MWNTs), single-walled carbon nanotube (SWNTs), and MWNTS-carboxylic (the MWNTs were treated with carboxylic acid). They are produced by Shenzhen Nanotech Port Co., Ltd., Shenzhen, China, and the characteristics of them are listed in Table I.

Prior to preparation of nanocomposites, PA1010 were dried in a vacuum oven for 24 h at 80°C. The composites of PA1010 and CNTs were mixed in a Haake rheomix mixer at 220°C at 50 rpm for 10 min. A control PA1010 sample without nanotube was also processed in the Haake mixer under the same conditions for comparison. The composites studied are presented in Table II.

The thermal analysis measurements were done using PerkinElmer DSC-7 series differential scanning calorimeter (DSC). Crystallization tests were carried out both in isothermal conditions and in dynamic conditions. The instrument was calibrated with an indium standard, and all the measurements were conducted under a nitrogen atmosphere at a flow rate of 20 mL/min. For the isothermal testing, a sample of about 7 mg was first heated rapidly to 230°C at a scan rate of 80°C/min and held there for 5 min to remove prior thermal histories. Subsequently, the samples were cooled to the appropriate crystallization temperature, T_c, at a rate of 80°C/min. For the observation of the melting peak after crystallization, the samples were then heated to 230°C at a rate of 10°C/min. The heat generated during the development of the crystallization phase was recorded up to a vanishing thermal effect and analyzed according to the usual procedure to obtain the relative degree of crystlallinity, $X(t)$:

$$X(t) = \frac{X_c(t)}{X_c(t_\infty)} = \frac{\int_o (dH/dt)dt}{\int_o^\infty (dH/dt)dt} \quad (1)$$

where $X_c(t)$ is the absolute degree of crystallization at the time t; dH/dt is the rate of crystallization heat evolution at time t; t_0 is the time at which the sample attains isothermal conditions, as indicated by a flat base line after the initial spike in the thermal curve. Absolute degree of crystallinity of PA1010 and its composites was evaluated by means of the relationship

$$X_c(t) = \frac{\int_o (dH/dt)dt}{(1-\alpha)\Delta H_f^0} \quad (2)$$

where ΔH^0_f = 244 J/g is the heat of fusion for 100% crystalline PA1010 and α is the mass fraction of the filler in the composites.

For dynamic DSC testing, the samples of 7 mg were heated from 50 to 230°C at a rate of 20°C/min and maintained at this temperature for 5 min to eliminate any previous histories in the material. The then samples were cooled to 50°C at a scan rate of 20°C/min. Subsequently, the melting point (T_m) was measured by the temperature being raised to 230°C at a rate of 20°C/min. The exothermal curves of the heat flow as a function of temperature were recorded for later analysis.

TABLE II
The Samples of Nanocomposites Studied

Code	Filler	PA1010/Filler (mass ratio)
PA1010		100/0
PA1010-S	SWNTs	98/2
PA1010-M	MWNTs	98/2
PA1010-M-acid	MWNTs-carboxylic	98/2

RESULTS AND DISCUSSION

The equilibrium melting point

Prior to carrying out the quantitative analysis of crystallization behavior, the equilibrium melting temper-

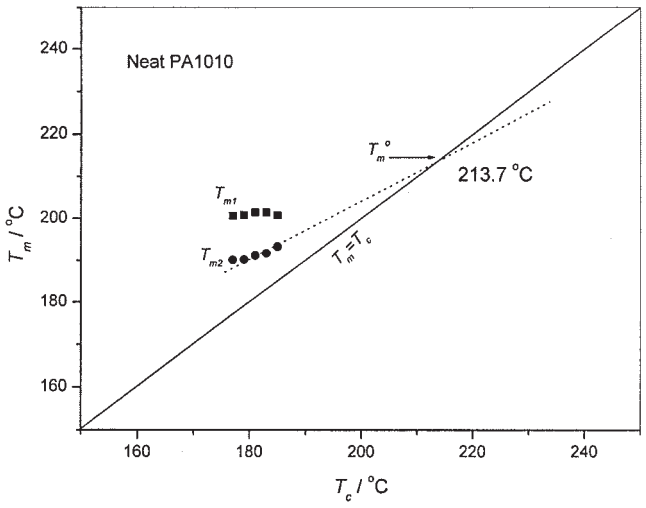

Figure 1 The equilibrium melting point of PA1010 measured from the isothermal crystallization process.

ature must be decided as exactly as possible. For instance, the thermodynamic parameter K_g is very sensitive to its value. According to Hoffman–Weeks's theory,[18] the equilibrium melting temperature can be attained only from DSC measurements.

The melting curves of neat PA1010 and its CNTs/PA1010 nanocomposites show two melting endothermic peeks. The high melting temperature T_{m1} is irrespective of crystallization temperature (T_c), which could be the result of recrystallization of the sample materials. The low melting temperature T_{m2} is correlated to T_c and increases with increase in T_c. The equilibrium melting point T_m^0 is obtained by the intersection of the straight line resulting from T_{m2} against T_c with the line $T_m = T_c$ using the Hoffman–Weeks's equation[19]

$$T_m = T_m^0(1 - 1/\gamma) + T_o/\gamma \quad (3)$$

where γ is the lamellar thickening factor, which describes the growth of lamellar thickness during crystallization. The obtained T_m^o of PA1010 is 213.7°C in Figure 1 dealt with the result published in literature.[20] T_m^o of CNTs/PA1010 nanocomposites are similar to those of pure PA1010 and the difference among these samples in Table II is less than 1°C.

Isothermal crystallization kinetic analysis

Figure 2 exhibits the plots of the relative crystallization degree versus time for PA1010 and its composites with CNTs in the isothermal crystallization process. It can be seen that all these curves have the same sigmoid shape except for the different crystallization temperature, T_c. Figure 2 reveals that the crystallization time becomes longer with increase in T_c for pure PA1010. A similar trend is observed in CNTs/PA1010 nanocomposites. However, CNTs/PA1010 nanocomposites complete the crystallization in less time than does pure PA1010 at the same crystallization temper-

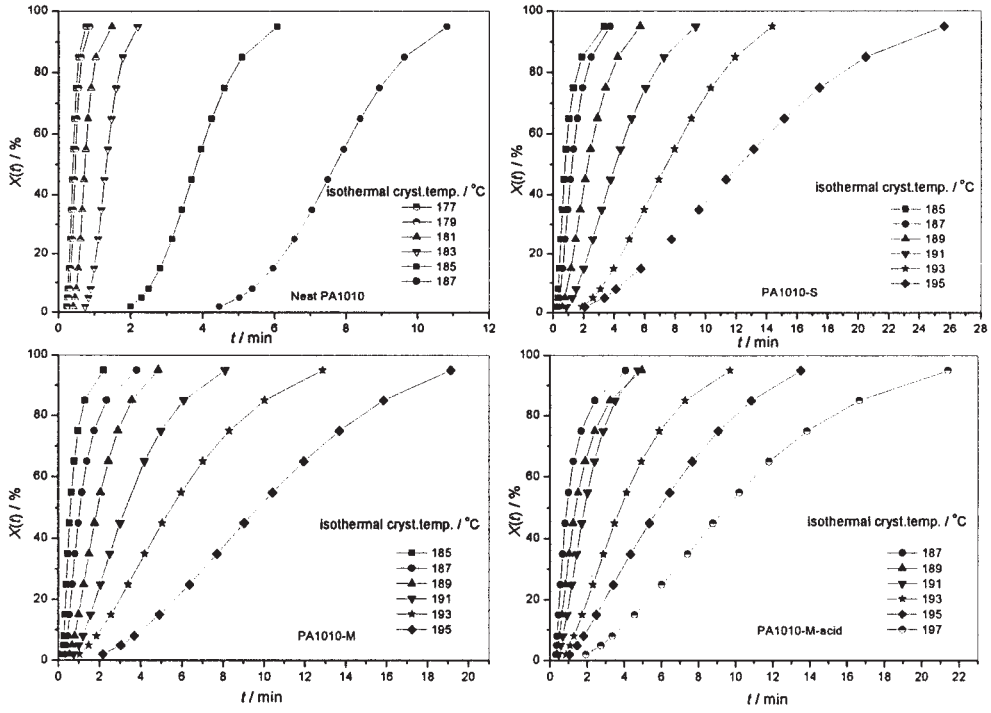

Figure 2 The relative degree of crystallinity versus time for isothermal crystallization of PA1010 and its composites.

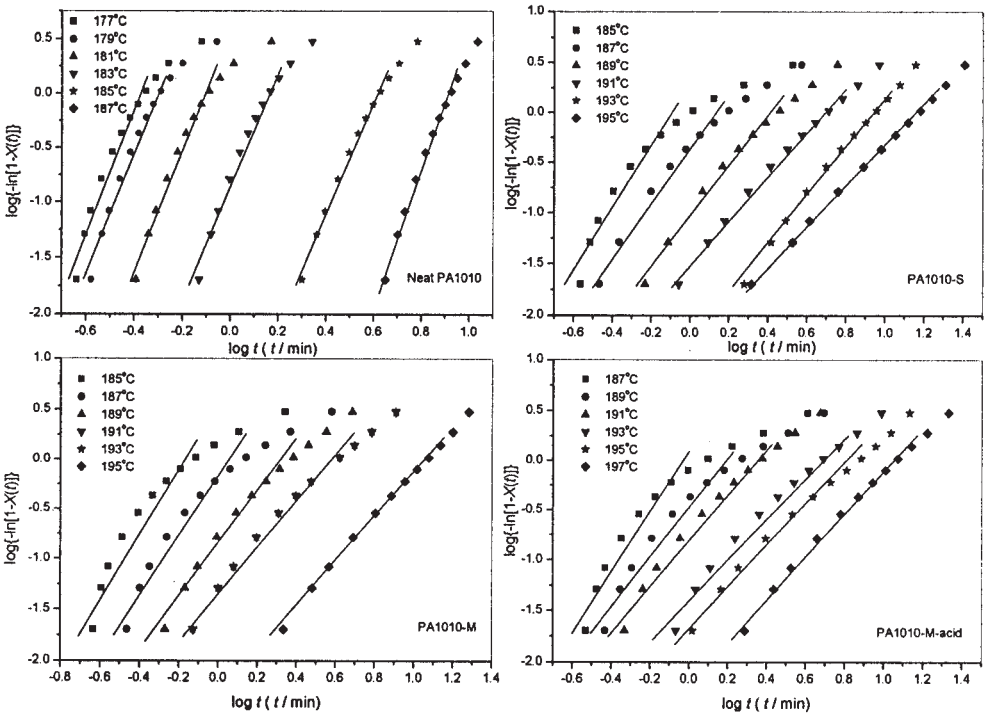

Figure 3 Plots of $\log\{-\ln[1 - X(t)]\}$ against $\log t$ for PA1010 and its nanocomposites under isothermal conditions.

ature, suggesting that the addition of CNTs accelerates the overall crystallization process.

To study the kinetics parameters for isothermal crystallization process, the Avrami equation is employed as follows[21,22]:

$$1 - X(t) = \exp(-Kt^n)$$

$$\log\{-\ln[1-X(t)]\} = \log K + n \log t \quad (4)$$

where $X(t)$ is the relative crystallization degree, t is the crystallization time, and n is the Avrami index. K is the crystallization rate constant, which depends on the nucleation and growth mechanism of the crystals.[23] Because of the complexity of the crystallization process, nucleation impossibly developed in a certain manner and transformation in the morphology of crystals may occur at different stages throughout the whole crystallization process. Hence, Avrami index n is usually not an integer but a decimal fraction and cannot precisely determine the mechanism of nucleation and growth of crystals. On the other hand, the Avrami equation, at present, still plays an important role in characterizing the kinetic theory of polymer isothermal crystallization.

Plots of $\log\{-\ln[1 - X(t)]\}$ against $\log t$ are linear at a low degree of crystallization and no change in the slope was observed until long times of conversion, as shown in Figure 3. The experiment data seem to fit the Avrami equation well. The values of K and n determined by the intercepts and slopes, respectively, of these straight lines are summarized in Table III. It is observed that the values of n vary from 3.8 to 5.1 for pure PA1010 and from 1.4 to 2.2 for CNTs/PA1010

TABLE III
Values of Crystallization Parameters of PA1010 and Its Nanocomposites (n, K, K_g)

Sample	T_c (°C)	n	K (min^{-1})	K_g (K^2)
PA1010	177	3.8	22.5	1.69×10^5
	179	4.2	16.5	
	181	3.9	2.3	
	183	4.2	2.1×10^{-4}	
	185	4.1	2.6×10^{-3}	
	187	5.1	2.1×10^{-5}	
PA1010-S	185	1.6	9.7×10^{-1}	8.19×10^4
	187	1.8	4.7×10^{-1}	
	189	1.8	1.5×10^{-1}	
	191	1.9	5.1×10^{-2}	
	193	2.2	9.1×10^{-3}	
	195	1.9	5.4×10^{-3}	
PA1010-M	185	1.8	1.6	7.79×10^4
	187	1.7	6.0×10^{-1}	
	189	1.8	2.0×10^{-1}	
	191	1.8	8.6×10^{-2}	
	193	1.8	3.5×10^{-2}	
	195	2.1	6.6×10^{-3}	
PA1010-M-acid	187	1.4	7.5×10^{-4}	5.77×10^4
	189	1.5	4.1×10^{-1}	
	191	1.8	2.3×10^{-1}	
	193	1.7	7.3×10^{-2}	
	195	1.6	4.2×10^{-2}	
	197	1.9	9.7×10^{-3}	

nanocomposites. Liu and Wu[24] found that the addition of MMT into polyamide 6 causes an increase in n value, compared with neat polyamide 6. They thought that the change in the values of n before and after introducing the MMT suggests that MMT layers dispersed in the matrix influence the mechanism of nucleation and crystal growth.[24] Liu and Yan[25] also observed a similar phenomenon when they studied the crystallization behaviors of polyamide 1010/montmorillonite nanocomposites.

The fact that the Avrami index n changed largely when CNTs are incorporated into PA1010 indicates that the CNTs seem to significantly affect the growth mechanism for the nanocomposites. For the CNTs/PA1010 nanocomposites, the value of n is almost between 1 and 2, implying that the crystals may grow as fibrils (one-dimensional growth). For neat PA1010, the value of n is approximately from 3 to 4, reflecting the spherulitic growth of the crystals (three-dimensional growth). The plots show linear deviation at a high crystallization degree in Figure 3, probably because of secondary crystallization, i.e., the impingement of spherulites with one another or overlapping of primary nucleation and crystal growth.

As expected, the K values of nanocomposites are higher than those of pure PA1010 at identical situation. Moreover, the K value of PA1010M-acid is larger than those of the other two nanocomposites, and especially, the K value of PA1010-S is minimum for nanocomposites, though it is higher than that of pure PA1010. When the values of n and K are known, $t_{1/2}$ (the half-time of crystallization) can be calculated through the following equation:

$$t_{1/2} = \left(\frac{\ln 2}{K}\right)^{1/n} \tag{5}$$

which is inferred from eq. (4) and also can be directly read from Figure 2. The $t_{1/2}$ values of pure PA1010 and its nanocomposites are listed in Table IV, together with the other characteristics of crystallization.

To compare with neat PA1010, the $t_{1/2}$ values of nanocomposites are greatly shortened at the same T_c, confirming that the introduction of CNTs created a strong nucleation effect and an acceleration of crystallization of PA1010 again. From Table IV, we also see that the values of $t_{1/2}$ and $t_{\max}$ (the time at maximum crystallization rate) increase with increase in T_c. $t_{\max}$ can be calculated through the equation

$$t_{\max} = \left(\frac{n-1}{nK}\right)^{1/n} \tag{6}$$

More difficult crystallization caused by the lower supercooling temperature ΔT ($T_m^o - T_c$) and larger free energy of nucleation may be responsible for the increase in $t_{1/2}$ when T_c moves up to higher temperature. However, the $t_{1/2}$ value of PA1010M-acid is minimum when compared with those of PA1010-S and PA1010M at the same condition, suggesting that the crystallization rate of PA1010M-acid is maximum among the three kinds of nanocomposites. This is well in accordance with the result of K values that we obtained earlier.

TABLE IV
Values of Crystallization Parameters of PA1010 and Its Nanocomposites ($t_{1/2}$, t_{max}, H_c)

Sample	T_c (°C)	$t_{1/2}$ (min)	t_{max} (min)	ΔH_c (J/g^{-1})
PA1010	177	0.40	0.41	−46.563
	179	0.47	0.48	−43.479
	181	0.74	0.75	−39.956
	183	1.33	1.35	−32.011
	185	3.91	3.98	−31.308
	187	7.69	7.92	−28.782
PA1010-S	185	0.81	0.55	−33.039
	187	1.24	0.97	−33.922
	189	2.34	1.83	−31.386
	191	3.95	3.23	−28.488
	193	7.17	6.43	−13.765
	195	12.87	10.54	−11.604
PA1010-M	185	0.62	0.48	−31.135
	187	1.08	0.80	−33.966
	189	1.99	1.56	−29.689
	191	3.19	2.49	−29.176
	193	5.25	4.10	−20.647
	195	9.17	8.03	−17.135
PA1010-M-acid	187	0.95	0.50	−38.764
	189	1.42	0.87	−41.463
	191	1.85	1.44	−27.435
	193	3.76	2.77	−19.677
	195	5.77	3.93	−17.722
	197	9.46	7.74	−24.275

The kinetic theory of polymer crystallization developed by Hoffman[26] has been generally used to analyze experimental data concerning spherulite growth rate. In this theory, the growth rate of spherulites, G, is described by the following equation:

$$G = G_o \exp\left[-\frac{U^*}{R(T_c - T_\infty)}\right]\exp\left(-\frac{K_g}{fT_c\Delta T}\right) \tag{7}$$

where G_0 is the preexponential factor, which is generally assumed to be constant or proportional to the crystallization temperature, T_c; U^*, the activation energy for transport of polymer segments to the site of crystallization; R, the gas constant; and T_∞, a temperature somewhat below the glass transition temperature, T_g; at this temperature, the viscosity is infinite. ΔT is the degree of surpercooling ($\Delta T = T_m^o - T_c$). The quantity f is the correction factor for the heat fusion; it takes into account the temperature dependence of ΔH_f^0. Usually, the following expression is used for f:

$$f = \frac{2T_c}{T_m^o + T_c} \tag{8}$$

K_g, the nucleation factor, is given by

$$K_g = \frac{Zb_o\sigma\sigma_e T_m^o}{k\Delta H_f^o} \tag{9}$$

where k is the Boltzmann's constant; b_0, the layer thickness; T_m^o, the equilibrium melting point; ΔH_f^0, the theoretical enthalpy of fusion per unit mass; σ and σ_e, the surface energies of the lateral and fold surfaces, respectively; and Z, a coefficient that depends on the growth regime.

It has been shown that it is possible to use calorimetric data obtained in isothermal conditions to discuss the overall crystallization behavior according to nucleation theories.[27] In fact, the growth rate G is related to Avrami index n by the simple relation

$$G = CK^{1/n} \tag{10}$$

where C is a constant and K is the crystallization rate constant. Combination of eqs. (7) and (10) can give

$$\ln C + \frac{1}{n}\ln K = \ln G_o - \frac{U^*}{R(T_c - T_\infty)} - \frac{K_g}{fT_c\Delta T} \tag{11}$$

The plots of $\ln K/n + U^*/[R(T_c - T_\infty)]$ against $1/(fT_c\Delta T)$ for the PA1010 and its nanocomposites are shown in Figure 4. The experimental data fit the straight lines well. The slopes of the straight lines in the Figure give the K_g values as shown in Table III. From eq. (9), we can conclude that $\sigma\sigma_e$ is directly proportional to K_g. In the analysis of our experimental results using eq. (11), the U^* and T_∞ may be assigned as universal values of 6280 J/g and $T_g - 30$°C, respectively, T_g being the glass transition temperature. In this study, the T_g of PA1010 is taken as 58°C.[28] T_m^o and ΔH_f^0 of PA1010 are 214°C and 244 J/g, respectively.[20]

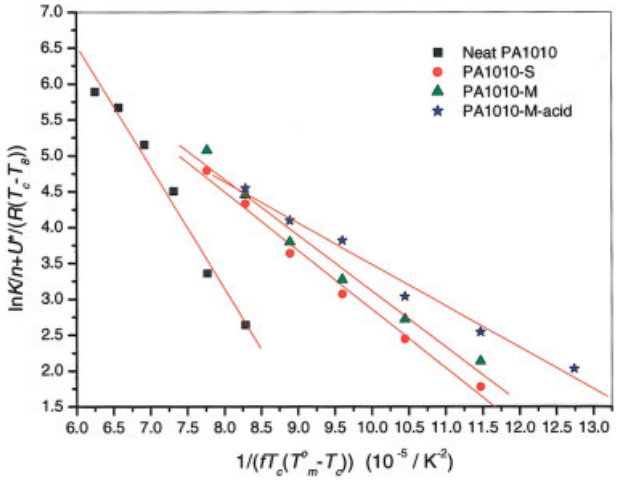

Figure 4 Plots of $\ln K/n + U^*/[R(T_c - T_\infty)]$ against $1/(fT_c\Delta T)$ for PA1010 and its nanocomposites. [Color figure can be viewed in the online issue, which is available at www.interscience.wiley.com.]

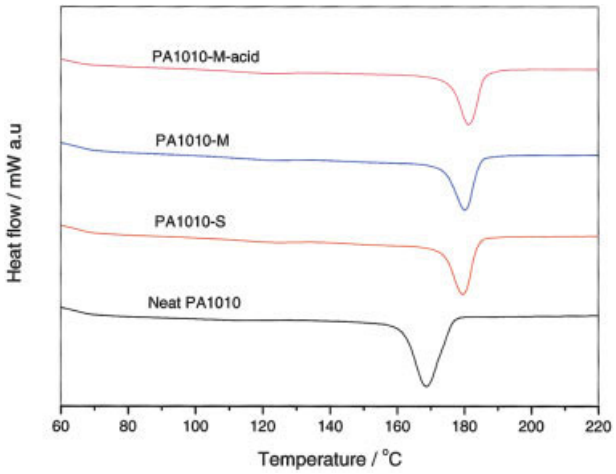

Figure 5 The curves for nonisothermal crystallization of PA1010 and its nanocomposites. [Color figure can be viewed in the online issue, which is available at www.interscience.wiley.com.]

These results show that the introduction of these CNTs to pure PA1010 decreases the lateral surface energies and then significantly enhances the crystallization rate of PA1010. Especially, MWNTs-carboxylic increases the crystallization rate more efficiently. We suggest that the significant enhancement in crystallization rate of PA1010 for PA1010-S and PA1010M is mainly attributed to the strong physical adsorption of PA1010 molecules onto the nanotube surface. For PA1010M-acid, the hydrogen-bonding interactions between chemically modified MWNTs and PA1010 mostly contribute to the increase in crystallization rate in addition to physical adsorption action.

Nonisothermal crystallization analysis

The effect of CNTs on the crystallization of PA1010 in CNTs–PA1010 blends was also analyzed in nonisothermal experiments. Although the treatment of nonisothermal crystallization is more complex, its study is of great interest, because these conditions are closer to industrial processing conditions. Figure 5 shows the dynamic thermograms obtained for neat PA1010 and its composites.

The observed dynamic crystallization behavior confirms the results obtained in isothermal tests regarding the positive effect of CNTs on the crystallization kinetics of PA1010. The values of T_c (crystallization peak temperature), T_0 (onset crystallization temperature), ΔW (half-width of crystallization peak), ΔH_c (the crystallization enthalpy), and T_m (melting temperature) of

TABLE V
Nonisothermal Crystallization Parameters of PA1010 and Its Nanocomposites

Sample	T_c (°C)	T_o (°C)	T_m (°C)	ΔW (°C)	ΔH_c (J/g)
PA1010	168.56	176.08	201.58	8.3	−65.22
PA1010-S	179.56	183.94	200.57	6.8	−53.49
PA1010-M	180.22	184.57	201.24	6.6	−51.52
PA1010-M-acid	181.20	185.99	201.56	6.0	−54.82

the crystallized samples (the DSC melting traces are not shown in this text) are given in Table V. As can be seen from Figure 5, the crystallization peaks shift to higher temperature with the presence of CNTs in PA1010. In addition, the crystallization peaks in CNTs/PA1010 composites are narrower than that of pure PA1010, implying a narrower crystallite size distribution in the nanocomposites as compared with that in neat PA1010 and a quicker crystallization process with the introduction of CNTs. High thermal conductivity of the CNTs as compared with that of the polymer, at least in part, may be responsible for the sharper crystallization peaks, as heat will be more evenly distributed in the samples containing the CNTs.[15]

Furthermore, from Table V, T_0 and T_c of nanocomposites are apparently higher than those of PA1010. For example, the difference of T_c value between PA1010M and PA1010 is over 10°C and that of T_0 is more than 8°C. This also indicates that the addition of CNTs enhances the nucleation rate of crystallization of PA1010. The ΔH_c values of nanocomposites are smaller than that of the PA1010, which means a decrease in the degree of crystallinity. In the meantime, no significant changes were observed on the melting temperature of the PA1010.

CONCLUSIONS

The isothermal melt-crystallization kinetics and nonisothermal crystallization behavior of CNTs/PA1010 nanocomposites were investigated by DSC. It has been demonstrated that the incorporation of CNTs affects the crystallization behavior of PA1010. The isothermal and nonisothermal crystallization data show that the half-time of crystallization, $t_{1/2}$, and the time at maximum crystallization rate, t_{max}, of CNTs/PA1010 composites are significantly reduced, as well as the nucleation factor K_g; the values of crystallization rate constant K for nanocomposites are also larger than that of neat PA1010; the T_c of CNTs/PA1010 composites shift to higher temperature in nonisothermal conditions. These confirm that the CNTs accelerate the nucleation and crystal growth of PA1010. In particular, the nucleation effect and acceleration in crystallization process for PA1010M-acid are most evident and those of PA1010-S are minimum in three types of CNTs. We also deduced that a fibrillar morphology instead of the usually obtained spherulitic morphology for neat PA1010 is developed in these composites. This seems to be supported by the kinetic data according to Avrami's theory: n, related to the dimensionality of crystal structure, is lower for CNTs/PA1010 composites than for pure PA1010. The energies of crystallization of PA1010 and its nanocomposites calculated under isothermal conditions supported the positive effect on crystallization process of PA1010 in presence of CNTs.

References

1. Qu, L.; Lin, Y.; Hill, D. E.; Zhou, B.; Wang, W.; Sun, X.; Kitaygorodskiy, A.; Suarez, M.; Connell, J. W.; Allard, L. F.; Sun, Y. P. Macromolecules 2004, 37, 6055.
2. Bianco, A.; Prato, B. Adv Mater 2003, 15, 1765.
3. Moore, E. M.; Ortiz, D. L.; Marla, V. T.; Shambaugh, R. L.; Grady, B. P. J Appl Polym Sci 2004, 93, 2926.
4. Sreekumar, T. V.; Liu, T.; Min, B. G.; Guo, H.; Kumar, S.; Hauge, R. H.; Smalley, R. E. Adv Mater 2004, 16, 58.
5. Liu, T. X.; Phang, I. Y.; Shen, L.; Chow, S. Y.; Zhang, W.-D. Macromolecules 2004, 37, 7214.
6. Seo, M.-K.; Park, S.-J. Chem Phys Lett. 2004, 395, 44.
7. Mo, Z. S.; Meng, Q. B.; Feng, J. H.; Zhang, H. F.; Chen, D. L. Polym Int 1993, 32, 53.
8. Varga, J.; Menyhard, A. J Therm Anal Cal 2003, 73, 735.
9. Lopez Manchado, M. A.; Biagiotti, J.; Torre, L.; Kenny, J. M. J Therm Anal Cal 2000, 61, 437.
10. Pegoretti, A.; Penati, A. Polymer 2004, 45, 7995.
11. Di Maio, E.; Iannace, S.; Sorrentino, L.; Nicolais, L. Polymer 2004, 45, 8893.
12. Zhang, Q.-X.; Yu, Z.-Z.; Xie, X.-L.; Mai, Y.-W. Polymer 2004, 45, 5985.
13. Mucha, M.; Królikowski, Z. J Therm Anal Cal 2003, 74, 549.
14. Valentini, L.; Biagiotti, J.; Kenney, J. M.; Santucci S. J Appl Polym Sci 2003, 87, 708.
15. Bhattacharyya, A. R.; Sreekumar, T. V.; Liu, T.; Kumar, S.; Ericson, L. M.; Hauge, R. H.; Smally, R. E. Polymer 2003, 44, 2373.
16. Valentini, L.; Biagiotti, J.; Kenney, J. M.; López Manchado, M. A. J Appl Polym Sci 2003, 89, 2657.
17. Assouline, E.; Lustiger, A.; Barber, A. H.; Cooper, C. A.; Kliein, E.; Wachtel, E.; Wagner, H. D. J Polym Sci Part B: Polym Phys 2003, 41, 520.
18. Hoffman, J. D.; Weeks, J. J. J Chem Phys 1962, 37, 1723.
19. Hoffman, J. D.; Weeks, J. J. J Natl Bur Stds 1962, 66, 13.
20. Feng, J. H.; Mo, Z. S.; Chen, D. L. Chin J Polym Sci 1990, 8, 62.
21. Avrami, M.; J Chem Phys 1940, 8, 212.
22. Avrami, M.; J Chem Phys 1941, 9, 177.
23. Schultz, J. M. Polymeric Materials Science; Prentice-Hall: New York, 1981.
24. Liu, X. H.; Wu, Q. J. J Eur Polym 2002, 38, 1383.
25. Liu, Z. J.; Yan, D. Y. Polym Eng Sci 2004, 44, 861.
26. Hoffman, J. D. Polymer 1983, 24, 3.
27. Hoffman, J. D.; Davies, G. T.; Lauritizen, J. L., Jr. In Treatise in Solid State Chemistry; Hannay, N. B. Ed.; Plenum: New York, 1976; Vol. 3, Chapter 7.
28. Feng, J. H.; Zhang, L. H.; Chen, D. L. Radial Phys Chem 1991, 38, 105.